View metadata, citation and similar papers at core.ac.uk

brought to you by CORE

provided by Archivio istituzionale della ricerca - Università di Palermo

Semiconductor electrochemistry approach to passivity and passivity breakdown of metals and metallic alloys

F. Di Quarto and M. Santamaria

A critical appraisal of the use of the theory of semiconductors in characterising passive films on metals and alloys is provided, with special emphasis on the use of Mott–Schottky theory for the location of characteristic energy levels of the passive film–electrolyte junction. Some inconsistencies between theory and experimental results in the case of thin passive films are discussed together with possible alternative ways for overcoming such problems. The role of semiconducting properties in determining the pitting behaviour of passive films on W in solutions containing halide is presented and discussed. The validity of a recently proposed correlation between the solid state properties of passive films and the pitting potential is critically reviewed. CEST/2127

The authors are in the Dipartimento di Ingegneria Chimica dei Processi e dei Materiali, Viale delle Scienze 90128, Palermo, Italy (diquarto@dicpm.unipa.it). *Manuscript received 11 December 2003; accepted 19 January 2004.*

Keywords:

© 2004 IoM Communications Ltd. Published by Maney for the Institute of Materials, Minerals and Mining.

INTRODUCTION

The first experimental report on the then unknown 'semiconducting' properties of passive films on metals can be traced to Becquerel's study of photoeffects at metal/electrolyte interfaces dating from the first half of the 19th century.[1] However, there is no doubt that a systematic semiconductor based approach to the properties of passive films is attributable to the seminal papers of Mott[2] and Schottky[3] on the rectifying properties of metal/semiconductor contacts (copper/cuprous oxide).

However, apart from the pioneering work of Garrett and Brattain[4] in the mid 1950s, the systematic use of semiconductor theory for interpreting the kinetics of electron and ion transfer reactions (ETR and ITR) at passive metal/electrolyte interfaces dates back to the advent of the Gerischer's theory.[5]

In this short historical excursus, the classical papers of Dewald[6] deserve particular mention. These demonstrated the validity of Mott–Schottky (M–S) analysis of the impedance data at a single crystal ZnO/electrolyte interface for the location of the characteristic energy levels of a semiconductor/electrolyte (SC/El) junction. This work will be discussed further in the following pages owing to its tremendous impact on the promulgation of M–S analysis for characterising the semiconducting passive film/electrolyte interface.

As for the state of the art in studies of the electrochemistry of semiconductors during the mid 1960s, an excellent presentation can be found in the classical book by Myamlin-Pleskov.[7] From the point of view of passivity studies, it is interesting to recall a sentence from the appendix of another such book: 'The important problem remains of extending the theoretical concepts and experimental investigation methods to polycrystalline semiconductors, in particular, oxide films on so-called barrier metals and to oxide and sulfide electrodes and also to use the concepts of the electrochemistry of semiconductors for investigating the phenomena of the passivation of metals'.[8]

This last task was initially undertaken by Oshe and Rozenfel'd[9] who proposed characterisation of the nature of passive films on metals and alloys by using a photopotential method initially proposed by Williams[10] for bulk semiconductors. Some applications of such a method in passivity studies can be found in Refs. 11 and 12 and in other references therein. The inadequacy of Oshe and Rozenfeld's method in characterising complex metal/oxide/electrolyte interfaces was first shown by Hackerman *et al.*[13] This fact and the onset of more refined theories of photocurrent generation at illuminated semiconductor/electrolyte interfaces in the mid 1970s[14] rendered obsolete Oshe and Rozenfeld's method of characterisation of passive metal/electrolyte interfaces.

In fact as a result of an intensive research effort on the photoelectrochemical behaviour of semiconductor electrodes, aimed at harvesting solar energy by photoelectrochemical solar cells, different electrochemical techniques started to be exploited as analytical tools for *in situ* characterisation of semiconductor/electrolyte interfaces.[15–17] In many cases the investigated photoelectrodes were oxides so that it was evident to electrochemists that passive films and corrosion layers having semiconducting or insulating behaviour could be scrutinised by using the same techniques as those used for studying semiconductor/electrolyte interfaces.[18–20] Against this background, impedance and photoelectrochemical techniques, such as electrochemical impedance spectroscopy (EIS) and photocurrent spectroscopy (PCS), have gained much support for investigation of the physicochemical properties of passive layers.[21–24] The combined use of these techniques allows, in principle, the acquisition of information on the electronic properties of passivating layers as well as on the energetics of passive film/electrolyte junctions.

This paper reviews some older and some more recent results that help to provide a critical appraisal of the use of techniques and theories valid for crystalline semiconductors to characterise very thin passive films. Some inconsistencies arising from the extension of the theory of bulk crystalline semiconductors to amorphous or microcrystalline thin passive films will be discussed and it will be demonstrated how, in some cases, a different theoretical approach can provide a better answer or deeper insight into the semiconducting behaviour of passive films. Finally, both recent and older pitting models based on the theory of semiconductors will be presented and discussed briefly on the basis of the authors' own experimental results and data from the published literature.

THEORETICAL BACKGROUND

The physicochemical characterisation of passive films and corrosion layers is important for comprehension of the corrosion behaviour of metals and alloys. More importantly the location of characteristics energy levels of metal/passive film and passive film/electrolyte junctions is a preliminary task for understanding the kinetics of ITR and ETR at

CES (gamma) CES36636.3d 12/2/04 15:07:47 Rev 7.51n/W (Jan 20 2003)

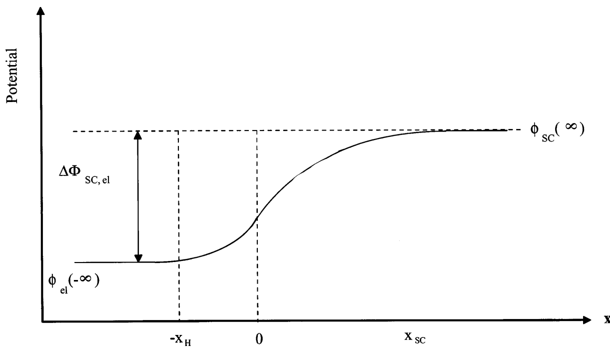

1 Schematic galvanic potential distribution across an n type semiconductor/electrolyte interface in the absence of specific absorption of ions in solution

passive film/electrolyte interfaces. In fact both ITR and ETR are controlled by (i) the energetics of the metal/film and film/electrolyte interfaces; and (ii) the electronic properties of the passive film.

With very few exceptions, most passive layers grown on metals and alloys behave like semiconducting or insulating materials. Accordingly, widespread use has been made of the theory of crystalline semiconductors to discuss the behaviour of passive film/electrolyte junctions. Such an extension is not always critically checked by taking into account whether the hypotheses underlying the theory of crystalline bulk semiconductors are also valid in the case of thin passive films often displaying behaviour typical of amorphous or poorly crystallised materials.[25]

For a better understanding of the different behaviours of crystalline and amorphous materials separate discussions will follow on the impedance and photoelectrochemical behaviours of selected systems which help in the derivation of a unified approach to the electrochemical and photoelectrochemical behaviour of crystalline and amorphous semiconducting passive films.

Figure 1 shows the schematic galvanic potential distribution across an n type semiconductor/electrolyte interface in the absence of the specific absorption of ions in solution. According to Fig. 1 the total potential drop across the interface is given by

$$\Delta\Phi_{SC/El} = \{\phi_{SC}(\infty) - \phi_{SC}(0)\} + \{\phi_{SC}(0) - \phi_{SC}(-\infty)\} \quad (1)$$

where the term in the first brackets of equation (1) represents the galvanic potential drop from the bulk (zero electric field) to the surface of the semiconductor/electrolyte junction, and the term in the second brackets is the galvanic potential drop occurring into the compact and diffuse double layer (if any) of the electrolytic solution. In the presence of concentrated electrolyte the diffuse double layer is missing and the previous equation can be rearranged as

$$\Delta\Phi_{SC/El} = \Delta\Phi_{SC} + \Delta\Phi_{H} \quad (2)$$

where $\Delta\Phi_{SC}$ and $\Delta\Phi_{H}$ represent the potential drop into the semiconductor and the Helmholtz double layer, respectively.

The region of semiconductor necessary for screening the potential drop $\Delta\Phi_{SC}$ defines the space charge region: X_{SC}. The width of the space charge region in crystalline semiconductors changes with the potential drop according to the following equation

$$X_{SC} = X^0_{SC}\left(|\Delta\Phi_{SC}| - \frac{kT}{e}\right)^{0 \cdot 5} \quad (3)$$

where X^0_{SC} represents the space-charge width into the semiconductor electrode at 1 V of band bending and its value depends on the concentration of mobile carriers into the semiconductor. In the hypothesis of completely ionised donors (for n type) or acceptors (for p type) the expression

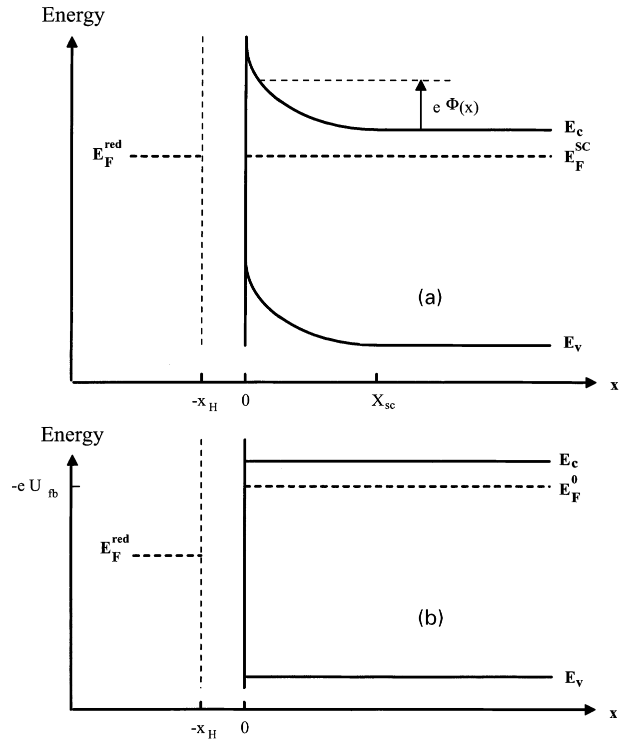

a under slight depletion ($X_{SC}>0$); *b* under flat band conditions ($X_{SC}=0$)

2 Schematic diagram of energy versus distance for an n-type semiconductor/electrolyte junction

for such a characteristic length is given by

$$X^0_{SC} = \left(\frac{2\varepsilon\varepsilon_0}{eN_D}\right)^{0 \cdot 5} \quad (4)$$

where N_D (or N_A) is the donor (or acceptor) concentration in cm^{-3} and ε and ε_0 are the dielectric constant and vacuum permittivity of the semiconductor, respectively. By assuming as typical values for passive films a dielectric constant equal to 10 and a donor concentration of 10^{19} cm^{-3} a value for X^0_{SC} of about 100 Å $V^{-0 \cdot 5}$ is obtained.

Figures 2*a* and 2*b* show schematic diagrams of an n-type semiconductor/electrolyte junction in energy-distance coordinates under slight depletion ($X_{SC}>0$) and at flat band conditions ($X_{SC}=0$). An anodic $\Delta\Phi_{SC}>0$ (n type semiconductor) polarisation corresponds to the conditions depicted in Fig. 2*a* while $\Delta\Phi_{SC}=0$ (no potential drop within the semiconductor) corresponds to the special flat band condition, $U_E = U_{fb}$, shown in Fig. 2*b*. In terms of electrode potential U_E for a semiconductor that is not heavily doped, and in the absence of an appreciable density of electronic surface states (SS)

$$\Delta\Phi_{SC} = U_E - U_{fb}(\text{ref}) \quad (5)$$

where U_{fb}(ref) represents the flat band potential measured with respect to a reference electrode in the electrochemical scale.

LOCATION OF CHARACTERISTIC ENERGY LEVELS IN CRYSTALLINE PASSIVE FILM/ELECTROLYTE JUNCTIONS

The determination of the flat band potential is a preliminary task in determining the locations (energetics) of characteristic energy levels (E_C, E_V, E_F) of any semiconductor/electrolyte interface. Once the U_{fb} value is known with respect to a reference electrode, it is possible to locate the Fermi level of the semiconductor in the electrochemical

CES *(gamma)* CES36636.3d 12/2/04 15:08:04 Rev 7.51n/W (Jan 20 2003)

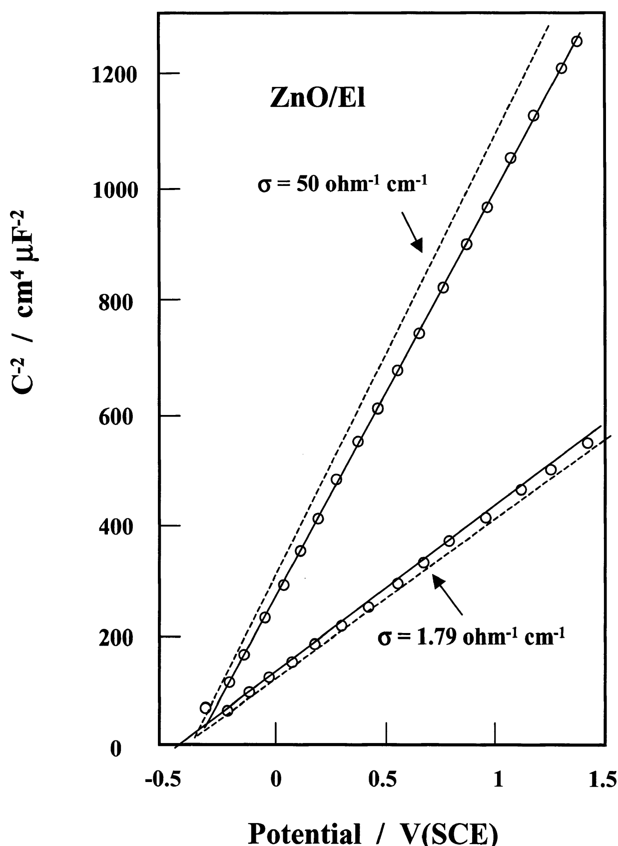

3 Mott–Schottky plots for two crystals under exhaustion conditions; the dotted lines represent the theoretical slope. At potentials more negative than −0·3 V, the capacitance increases exponentially. The intercepts of the linear plots afford a quantitative measure of the electrode potential at the flat band condition (from Ref. 6)

scale, E_F^0(El), by means of the relationship

$$E_F^0(\mathrm{El}) = -eU_{fb}(\mathrm{ref}) \quad (6)$$

The Fermi level in a semiconductor under electronic equilibrium will be located by assuming $E_F = E_F^0 - |e|\Delta\Phi_{SC}$, at any potential different of U_{fb}.

The U_{fb} location is usually determined by means of differential capacitance measurements of the semiconductor/electrolyte junction or from photocurrent versus potential curves. This last method is the only one available in the case of insulating films.

For semiconducting films, determination of the flat band potential is frequently based on the use of Mott–Schottky analysis of differential capacitance measurements of the junction. The validity of M–S theory has been tested rigorously for several crystalline semiconductor/electrolyte interfaces[6,26–31] since the very seminal work of Dewald on the ZnO/electrolyte interface, which greatly influenced the subsequent literature on semiconducting passive films (Fig. 3 and Table 1).

In the case of passive films, further complications can arise in the use of the classical approach owing to the possible presence of lattice disorder; the extreme thinness of the passive film; the extremely high donor/acceptor concentration; and geminate (i.e. twinned) recombination effects.

However, in the presence of crystalline films, as tacitly assumed without any further experimental support, the use of simplified M–S analysis can give rise to some inconsistencies with the simplifying hypothesis underlying the derived final equation.[6] It is perhaps not obvious to recall that the simplified Mott–Schottky equation

$$\frac{1}{C_{SC}^2} = \frac{2}{\varepsilon\varepsilon_0 N_D}\left(\Delta\Phi_{SC} - \frac{kT}{e}\right) \quad (7)$$

frequently used to derive the flat band potential and donor (or acceptor) density in passive films is obtained under a number of assumptions not always supported by the results derived by using the starting equation. It should be recalled that equation (7) is based on the following simplifying assumptions:

1. The semiconductor is homogeneously doped and the donors are completely ionised in the bulk.
2. The semiconductor is not degenerate so that Maxwell–Boltzmann statistics hold. This implies that the Fermi level in the bulk of the semiconductor is sufficiently far in energy ($>3kT$) from the conduction band edge (or from the valence band edge for p type semiconductors).
3. The electrode potential is quite anodic so that $\Delta\Phi_{SC} \gg kT/e$.

Where the previous conditions are satisfied the location of the remaining energy levels of the junction can be determined from the relationships valid for crystalline semiconductors

$$E_C = E_F^0 + kT \ln\left(\frac{N_C}{N_D}\right) \quad \text{for n type semiconductors (8a)}$$

$$E_V = E_F^0 - kT \ln\left(\frac{N_V}{N_A}\right) \quad \text{for p type semiconductors (8b)}$$

$$E_g = E_C - E_V \quad (9)$$

where E_C and E_V the conduction and valence band edges, respectively; N_C and N_V are the effective densities of states at the bottom of the semiconductor's conduction band and at the top of the semiconductor's valence band; N_D and N_A are the donor and acceptor concentrations in the semiconductor; and E_g is the band gap of the semiconductor.

For heavily doped semiconductors the first two assumptions are not valid so equations (7) and (8) cannot be used so straightforwardly without contradictions. In order to highlight this point it should be noted that the effective density of states (DOS) at the conduction (valence) band edge for n type (p type) semiconductors is given by[32]

$$N_C = 2M_C\left(\frac{2\pi m^* kT}{h^2}\right)^{3/2} \quad (10)$$

where M_C is the number of equivalent minima (maxima) in the conduction (valence) band, m^* is the effective mass for the DOS in the corresponding band, h = Planck's constant and the other symbols have their usual meanings. By assuming $M_C = 1$ and m^* is equal to the mass of a free electron m_0, we get $N_C = 2{\cdot}5 \times 10^{19}$ cm^{-3} at room temperature. This last value must be compared with the usual values reported for donor density N_D in passive films.

In the case of passive iron, from the analysis of Mott–Schottky plots, values of N_D ranging between 5×10^{20} and 2×10^{21} are often reported in the literature.[33–37] In order to

Table 1 Frequency dependence of capacitance relating to single crystal ZnO electrodes in contact with aqueous borate buffer 1 N recrystallised KCl (pH ≅ 8·5)

Frequency, Hz	Slope of C^{-2} vs V plot, cm^4 μF^{-2} V^{-1}	Flat band potential, V/SCE
100	626	−0·471
200	626	−0·471
1000	628	−0·470
5000	625	−0·483
10000	629	−0·441

Source: Ref. 6.

CES *(gamma)* CES36636.3d 12/2/04 15:08:06 Rev 7.51n/W (Jan 20 2003)

assume as valid the M–S analysis previously outlined it is necessary to hypothesise an effective DOS at E_C in the order of 1×10^{22} cm^{-3}. From such a figure we can derive a value of effective mass for DOS of passive films on iron ranging from 60 to 20 for $1 < M_C < 5$. A value of effective mass around 20 is not unusual for bulk semiconductor oxides of transition metals,[38] but it should be taken with some caution in the absence of direct measurements of such a parameter in passive films on iron and by considering that this still high value corresponds to a rather high value of M_C.

More importantly, in the presence of such a large donor density, it is not excusable to neglect the shift of flat band potential and the influence of the potential drop in the Helmoltz double layer. Both effects have been discussed in the literature[39–41] and they should be taken into account for the correct location of the characteristic energy levels and a better understanding of the kinetics of charge transfer at the passive film/electrolyte interface.

As for the location of the flat band potential, the assumption of neglecting the contribution of Helmoltz capacitance to the measured capacitance values can seriously affect the value of flat band potential. In fact, the relationship between the intersection of the M–S plot with the potential axis, U_0, and the flat band potential value is as follows

$$U_{fb} = U_0 - \frac{kT}{e} + \frac{\varepsilon\varepsilon_0 e N_D}{2C_H^2} \quad (11)$$

The required correction in the U_{fb} value remains negligible as long as the dielectric constant ε and donor density N_D are small but it becomes important as both ε and N_D increase close to values such as those reported previously for passive iron. By substituting the value of dielectric constant usually reported for passive iron ($\varepsilon = 15$) and an average N_D value of 5×10^{20} between those ($1 \times 10^{20} - 1 \times 10^{21}$) reported in Refs 33–37, a difference between the flat band potential and the intersection voltage ranging between 0·13 V and 0·53 V is obtained for C_H values ranging between 20 and 10 μF cm^{-2}.

Moreover at high donor density the assumption, implicitly included in equation (5), that the potential drop in the compact Helmoltz double layer is constant as a function of the electrode potential and negligible with respect to the potential drop within the semiconductor is not tenable. The variation in the Helmoltz potential drop becomes an important fraction of the total potential drop and it could account for the non-linear M–S plots at lower band bending. At such high donor (acceptor) density the behaviour of the passive film electrolyte interface parallels that of a metal/electrolyte interface so that the assumption of fixed band edges must be relaxed.[40,41]

A second critical point in the application of classical M–S analysis to passive films comes from the strong frequency dependence usually observed in the differential capacitance values of the junctions which considerably affects both the slope (N_D, N_A) and the flat band potential values (see Fig. 7 of Ref. 37). As for the origin of the frequency dispersion in crystalline semiconductor/electrolyte junctions, a detailed analysis of possible sources has been performed in Refs 42,43 and in references contained therein and, therefore, it will be omitted here. However, it must be mentioned that frequency dependent capacitance values are anticipated in the case of amorphous semiconducting materials.[25] This aspect will be revisited later.

Photocurrent spectroscopy (PCS) location of U_{fb} and E_g in crystalline semiconductor/electrolyte junctions

In view of all these complications, data for the characteristic energy levels of junctions of passive films grown on iron, chromium, nickel and their alloys (stainless steels) must be regarded with great caution. In these cases it may be reasonable to get an estimate of the flat band potential value of the junction by using photocurrent vs potential curves at different wavelengths. This last method is the only one available for insulating films but it can also be useful for semiconducting films in the presence of strongly variable U_{fb} values derived from M–S analysis at different AC frequencies.

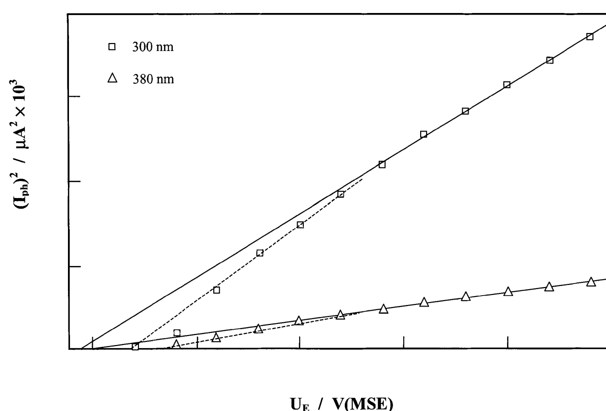

4 $(I_{ph})^2$ versus U_E plots recorded for a WO_3 film grown at 8 mA cm^{-2} in a 0·1 N H_3PO_4 electrolyte at up to 100 V and crystallised for 3 h at 350°C under an argon atmosphere. Electrode surface area: 0·053 cm^2. Irradiating wavelengths = 300 nm and 380 nm. (*Solar Energy Materials*, 1985, 11, 419)

In fact according to the generalised Gartner–Butler equation it is possible to write the following expression for the photocurrent I_{ph} at illuminated crystalline semiconductor/electrolyte junctions

$$I_{ph} = \frac{S_t}{S_t + S_r} e\Phi_0 \alpha X_{sc}^0 \left(U_E - U_{fb} - \frac{kT}{e}\right)^{1/2} \quad (12)$$

In this equation: Φ_0 is the photon flux (cm^{-2} s^{-1}) entering the semiconductor after light reflection losses; α is the light absorption coefficient at the impinging wavelength; and $S_t/(S_t + S_r)$ accounts for the ratio between the minority carriers transfer reaction rate S_t and the total recombination rate S_r. At high band bending such a ratio goes to 1 and it is possible to obtain the flat band potential by extrapolating to zero photocurrent a plot of I_{ph}^2 versus U_E under a high depletion regime (Fig. 4). In the presence of a low recombination rate the onset photocurrent potential V^* could provide a close estimate of the flat band potential. This last value is expected to be coincident or more anodic (cathodic) than the U_{fb} value of an n type (p type) semiconductor/electrolyte junction.

As for the semiconducting passive film/electrolyte interface (Ref. 25 and references therein) it has been shown that by irradiating the junction with photons having energy higher than the optical band gap of the film the measured photocurrent can be interpolated by a power law $(I_{ph})^n$ versus U_E whose intercept with the potential axis provides an approximation of the U_{fb} value. Moreover, frequently the onset photocurrent potential is not very far from the U_{fb} value obtained by M–S analysis.

This is evident in Fig. 5, which shows the I_{ph} versus U_E plot for an iron passive film grown potentiostatically in borate buffer solution. From such a plot it emerges that the onset photocurrent potential is not very far from the U_{fb} values[37] measured from M–S plots after correction for the potential drop in the Helmholtz double layer capacitance. An expression for the photocurrent, valid both for insulating and semiconducting materials, which takes into account possible geminate recombination effects in low

CES (gamma) CES36636.3d 12/2/04 15:08:07 Rev 7.51n/W (Jan 20 2003)

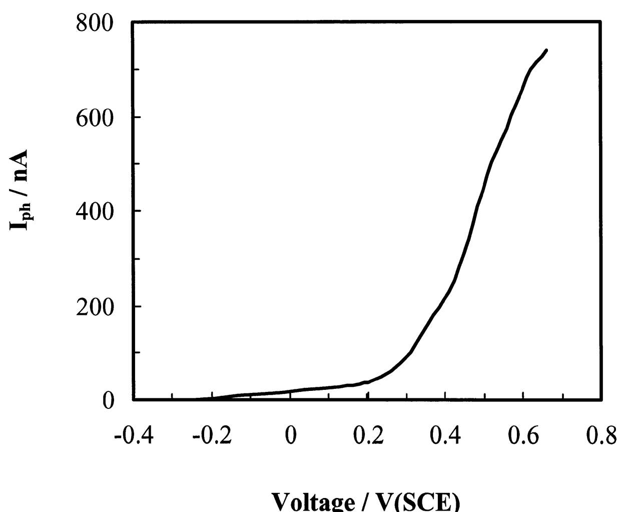

5 I_{ph} versus U_E plot for an iron passive film grown potentiostatically in borate buffer solution to V_f= 0·6 V(SCE). λ=380 nm; V_{scan}=5 mV s^{-1}

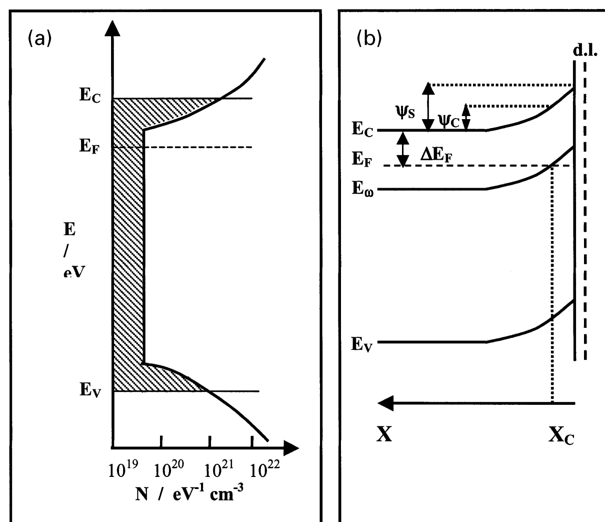

6 *a* Schematic density of states distribution in an amorphous semiconductor; *b* energetics at an amorphous semiconductor/electolyte junction

mobility materials has been previously published[25] and will be omitted here for sake of brevity.

The findings of Figs. 4 and 5 should encourage more confident use of photocurrent spectroscopy data for testing flat band potential values derived from M–S analyses of crystalline passive film/electrolyte junctions. Moreover PCS techniques provide an alternative way to locate the flat band potential in those cases where the behaviour of capacitance versus potential curves is not amenable to the simple (see also below) M–S analysis, or in the case of insulating passive films.

At constant potential, equation (12) also provides a direct proportionality between α and I_{ph} so that band gap values for semiconductor and passive films can be determined, thus allowing the complete location of energy levels of the junction.

LOCATION OF CHARACTERISTIC ENERGY LEVELS IN AMORPHOUS PASSIVE FILM/ ELECTROLYTE JUNCTIONS

The analysis of the impedance data outlined above is not valid in the case of amorphous or strongly disordered semiconducting passive films. It was shown some years ago that a different approach based on the theory of amorphous semiconductor (a-SC) Schottky barriers is able to explain the complex impedance behaviour of amorphous semiconducting passive film/electrolyte junctions.[44–46] According to the theory, the main difference in the impedance behaviour of amorphous semiconductor/electrolyte junctions stems from the difference in the electronic density of states (DOS) distribution occurring between amorphous and crystalline semiconductors. Figure 6 presents a schematic DOS distribution showing the presence of a large number of electronic states lying within the forbidden mobility gap (E_C-E_V) of the semiconductor. As a consequence, most of the electronic charge is now located below the Fermi level in localised states quite distant in energy from the conduction band mobility edge separating the extended states region from localised ones. According to the theory, [47–52] at variance with the case of crystalline semiconductors, the filled electronic states within the gap (Fig. 6*b*) do not instantaneously follow the imposed AC signal, but need a finite response time. This response time depends on their energy position with respect to the Fermi level and can be much longer than the period of the AC signal having an angular frequency ω. In fact the relaxation time τ for the capture/emission of electrons from electronic states E below E_F is assumed to follow the relationship

$$\tau=\tau_0 \exp\left(\frac{E_C-E}{kT}\right) \qquad (13)$$

where, at constant temperature, τ_0 is a constant characteristic of each material, usually ranging between 10^{-14} and 10^{-10} s. According to equation (13), by decreasing the energy of the localised state in the gap, τ increases sharply so that deep states (for which $\omega\tau\gg1$) do not respond to the AC signal.

By assuming a full response for states satisfying the condition $\omega\tau\ll1$ and a null response for states having $\omega\tau\gg1$, a sharp cutoff energy level E_ω separating states responding from those not responding to the signal, can be defined from the condition: $\omega\tau=1$.

The location of the cutoff level is found by imposing in equation (13) $\omega\tau=1$ for $E=E_\omega$, which gives

$$E_C-E_\omega=-kT\ln(\omega\tau_0) \qquad (14)$$

This condition occurs at some position within the barrier ($X=X_C$), which is a function of band bending and AC frequency (Fig. 6*b*). The intersection of the cutoff level E_ω with the Fermi level allows the point within the barrier X_C that separates two regions of the amorphous semiconductor to be located (Fig. 6*b*). The first one is for $X>X_C$, where all electronic states fully respond to the AC signal ($\omega\tau\ll1$), and the second one is for $X<X_C$, where they do not respond at all ($\omega\tau\gg1$). The corresponding band bending at X_C is given according to Fig. 6*b* by

$$|e|\psi_C=|e|\psi(X_C)=-kT\ln(\omega\tau_0)-\Delta E_F \qquad (15)$$

with $\Delta E_F=(E_C-E_F)_{bulk}$. It must be stressed that X_C is now a distance in the barrier which changes with changing frequency ω and band bending ψ_S. In particular X_C increases with increasing frequency, at constant polarisation, or with increasing polarisation at constant frequency. From the theory it emerges that the total capacitance is the sum of two series contributions coming from the $X<X_C$ and $X>X_C$ regions of the amorphous semiconductor. The contribution to the conductance comes mainly from the region around $X=X_C$ dividing the total response and null response regions. In the hypothesis of a constant density of states, the total capacitance is given by the sum of the two contributions

$$\frac{1}{C_P(\psi_S,\omega)}=\frac{1}{C(\psi_C,0)}+\frac{X_C}{\varepsilon\varepsilon_0} \qquad (16)$$

CES *(gamma)* CES36636.3d 12/2/04 15:08:07 Rev 7.51n/W (Jan 20 2003)

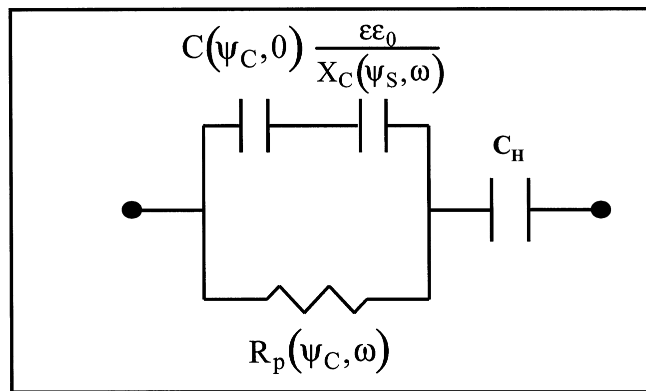

7 Equivalent circuit used to fit the impedance data. C_H is the Helmholtz capacitance and R_{sol} the electrolyte resistance (see text for other symbols)

where, for a density of states parameter N

$$C(\psi_C,0)=\sqrt{\varepsilon\varepsilon_0 e^2 N} \text{ and } X_C=\sqrt{\frac{\varepsilon\varepsilon_0}{e^2 N}}\ln\frac{\psi_S}{\psi_C}$$

After substitution the following relationship is obtained for the total capacitance in the low band bending regime

$$C_{LBB}(\psi_S,\omega)=\sqrt{\varepsilon\varepsilon_0 e^2 N}\left(1+\ln\frac{\psi_S}{\psi_C}\right)^{-1} \quad (17)$$

while the parallel conductance of the junction is given by

$$G_{LBB}(\psi_S,\omega)=\left(\frac{\omega\pi kT}{2}|e|\psi_C\right)\sqrt{\varepsilon\varepsilon_0 e^2 N}\left(1+\ln\frac{\psi_S}{\psi_C}\right)^{-2} \quad (18)$$

The analytical solutions for the admittance components of the junction have been derived under conditions that $\psi_S>\psi_C>3kT/e$ and at not too high band bending (low band bending regime, $e\psi_S<E_g/2$).[44–46]

It has been shown that $G(\psi_S,\omega)$ has a spectroscopic character with respect to the distribution of electronic states within the gap, while variations in DOS cause only minor changes in the $C(\psi_s,\omega)$ versus potential plots provided that the DOS varies little over an energy range of kT. In previous equations ε_0 is the vacuum permittivity, e the electronic charge, ε the film dielectric constant and ψ_s the potential drop inside the amorphous semiconductor, as above.

At variance with the M–S analysis, in the case of an amorphous semiconductor, a fitting procedure is required to obtain the flat band potential and density of states distribution around the Fermi level. As reported in previous works[44,45] the fitting must be carried out on both components of the admittance of the junction, after the correction of the measured quantities for the equivalent circuit shown in Fig. 7. The fitting procedure must be performed under the condition that at any employed AC frequency both the $1/C_{SC}$ versus ψ_S and the G_{SC} versus ψ_S plots give the same U_{fb} value, within an assigned uncertainty (in the present case, 0·05 V). Moreover an additional constraint arises from equation (15) requiring for ψ_C a variation of 59 mV per decade of frequency at room temperature (*see* below and Refs. 44, 45 and 53).

As previously reported[44,45] equation (15) must be used for locating the mobility edge, E_C (n type), or E_V (p type) once the ψ_C parameter and flat band potential U_{fb} have been obtained. With this aim an average τ_0 value of 10^{-12} s can be assumed in the absence of further information. The ability of previous admittance equations, in the low band bending approximation, to fit the experimental curves of different amorphous semiconductor passive film/electrolyte junctions has been tested in previous works.[44,45]

More recently the present authors have tested the ability of amorphous semiconductor Schottky barrier theory to fit the admittance data in a larger range of electrode potentials including the high band bending region when a deep depletion region at the surface of amorphous semiconductor/junctions appears.[54] In order to include the deep depletion region the previous equations have been modified as follows

$$\frac{1}{C_{HBB}(\omega,\psi_S)}=\frac{1}{\sqrt{\varepsilon\varepsilon_0 e^2 N}}\left(\ln\frac{\psi_G}{\psi_C}+\sqrt{1+\frac{2}{\psi_G}(\psi_S-\psi_G)}\right) \quad (19)$$

$$G_{HBB}(\omega,\psi_S)=\pi^2 f\,\frac{kT}{|e|\psi_C}\sqrt{\varepsilon\varepsilon_0 e^2 N}\times\left(\ln\frac{\psi_G}{\psi_C}+\sqrt{1+\frac{2}{\psi_G}(\psi_S-\psi_G)}\right)^{-2} \quad (20)$$

Equations (19) and (20) have been derived under the same conditions valid for the LBB expression and they coincide with the previous ones for $\psi_S\leqslant\psi_G$.

Figure 8*a* and *b* present the experimental admittance curves and their fits according to equations (19) and (20) for a thin ($\cong$25 nm) anodic film grown at a low scan rate (10 mV s^{-1}) on Nb in 1 M H_3PO_4 solution, while Fig. 9 shows the density of states distribution derived from the fitting of G and C as a function of the distance from the film/electrolyte interface ($X_{SC}=0$). In order to perform the fitting procedure a constant value of $\psi_G=1·6\pm0·1$ eV was assumed, in agreement with the measured band gap value, while a value of U_{fb} around $-0·05\pm0·025$ V(NHE) was assumed for the junction.[44,46,54] As for the fitting parameters U_{fb} and ψ_C, the same values were imposed for fitting the two components of the admittance with an uncertainty of 0·05 V in U_{fb} and less than 0·01 eV in ψ_C.

In order to expedite the fitting procedure, both components of the admittance were fitted initially in the LBB region then the fitting parameters were refined by a trial and error procedure, which assured the best fitting in the largest potential range covering the HBB region. In this second step the density of states parameter N was left to vary independently for the two components of the admittance. Account had to be taken of the fact that, according to the theory, a density of states value averaged over the space charge region is derived from the fitting of C, while the density of states that appears in the expression of G is that measured at energy level ($E_F-e\psi_C$) near the point X_C. The two density of states values apart, any possible source of inaccuracy, such as leakage currents through the junction which could affect the conductance values, are expected to coincide only in the hypothesis of constant and spatially homogeneous density of states within the gap and along the film. Location of the conduction band mobility edge was performed using equation (15) at a frequency ε within the investigated range and the corresponding ψ_C value was derived from the fitting process ($\Delta E_F=0·35$ eV with a τ_0 value of 10^{-12} s).

CES (gamma) CES36636.3d 12/2/04 15:08:10 Rev 7.51n/W (Jan 20 2003)

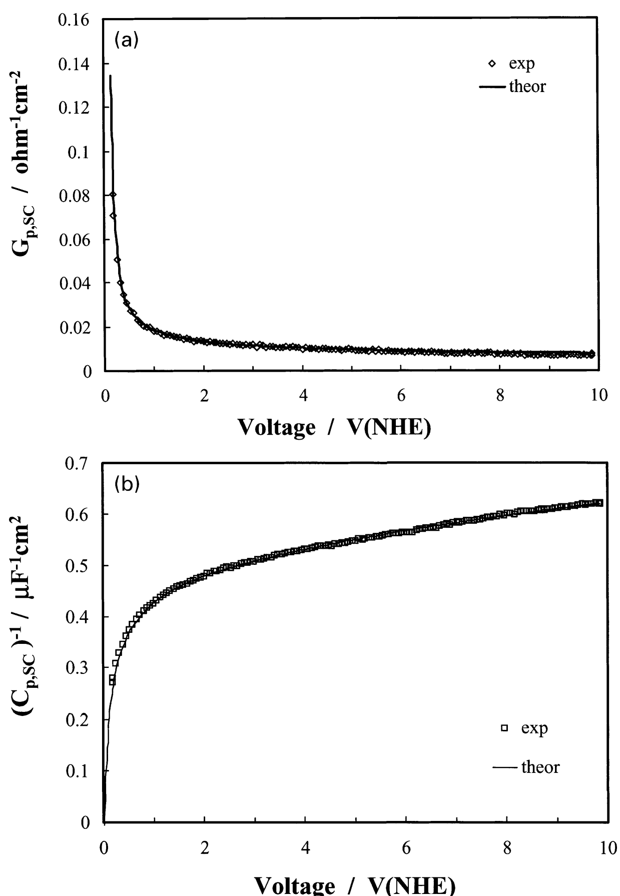

a G_p versus U_E; *b* $(C_p)^{-1}$ versus U_E

8 Fitting experimental admittance curves of a-Nb_2O_5 (V_f=9·64 V/NHE in 1 M H_3PO_4). Sol: 1 M H_3PO_4; f=10 kHz; scan rate=100 mV s^{-1}. Fitting parameters: ψ_C=0·085 V and U_{fb}=−0·025 V(NHE)

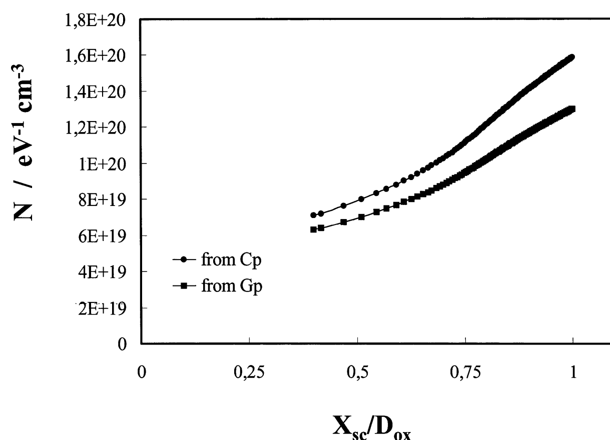

9 Spatial dependence of density of states derived from the fitted curves of Fig. 8. D_{ox} is the film thickness (≅25 nm)

PHOTOCURRENT SPECTROSCOPY (PCS) APPROACH TO THE LOCATION OF U_{FB} OF AMORPHOUS PASSIVE FILM/ELECTROLYTE JUNCTIONS

As previously mentioned for crystalline materials, a different way to locate the flat band potential of amorphous passive film/electrolyte junctions is based on the use of the photocurrent versus potential curves. Such a method allows an approximate estimation to be made of the U_{fb} value of the junction by determining, in a suitable way, the zero photocurrent potential of the junction.

In previous works it has been shown that in the case of amorphous materials, owing to the low mobility of injected photocarriers and the presence of electric fields that are not too high, the photocurrent versus potential curves become both field and wavelength dependent due to the presence of geminate recombination effects.[25] In these cases it has been shown that the zero photocurrent potential can be derived by fitting an expression of the photocurrent as a function of the photon energy and electric field that also accounts for the geminate recombination effects.[25] It has been shown that under steady state conditions the following general expression can be written for the photocurrent in an amorphous semiconductor as a function of the space charge region width, X_{SC}, and electric field[25]

$$I_{ph}=e\Phi_0\frac{\alpha L_d}{1+\alpha L_d}\left[1-\exp\left(-X_{SC}\frac{1+\alpha L_d}{L_d}\right)\right]\eta_g(r_0,F_{av}) \quad (21)$$

where $\eta_g(r_0, F_{av})$ is the efficiency of generation of free carriers in the presence of geminate recombination effects; L_d is the drift length of the photocarrier ensemble in the average field approximation

$$L_d=\mu\tau F_{av} \quad (22)$$

with μ and τ representing the drift mobility and the lifetime of the photocarrier ensemble respectively, and F_{av} the mean electric field in the amorphous superconductor.[25]

From equation (21) it is possible to derive the photocurrent for the amorphous insulator/electrolyte junction by substituting the film thickness d_f for the space charge region X_{SC} and by using the usual expression for the electric field in an insulator, $F_{av}=(U_E-U_{fb})/d_f$, in the absence of charge carrier trapping phenomena.[25]

The variation of the efficiency of generation with the electric field and photon energy, through r_0, can account for the dependence on the incident photon energy of the photocurrent versus potential curves. This last aspect has been discussed in depth both for semiconducting (a-WO_3 and a-TiO_2) and insulating (a-Ta_2O_5) anodic films in previous work[25] and it will be omitted here.

BREAKDOWN AND PITTING OF PASSIVE FILMS

The mechanism of failure of passive films is one of the most investigated issues in the electrochemistry of metals and in corrosion science.[55] This is due to its practical importance in determining the final film thickness during the anodising process of metals in solutions, as well as for improving the corrosion protection of metallic structures in different environments.

With regard to the mechanism of failure during the anodising process it is widely accepted that different mechanisms can operate depending on the nature of the anodising metal and the electrolytic solution. In spite of a risk of oversimplification, the term 'breakdown' (mechanical or electrical) will be used for any film failure occurring in the absence of typical pitting morphology, while the term 'pitting' will be used for any failure of the passive film associated with the occurrence of pitting events.

The mechanical breakdown of a passive film displays some typical features in the potential versus time curves at constant current density, which differentiates this mechanism from electrical breakdown.[56,57] It seems reasonable to exclude, as a first approximation, any direct influence of the semiconducting properties on the mechanical failure of passive films, although some interference between the electrical and mechanical breakdown phenomena can occur, as shown by the present authors some years ago for amorphous WO_3. Very recently, the possibility of void formation within the passive film, with oxygen trapping inside such

CES (gamma) CES36636.3d 12/2/04 15:08:11 Rev 7.51n/W (Jan 20 2003)

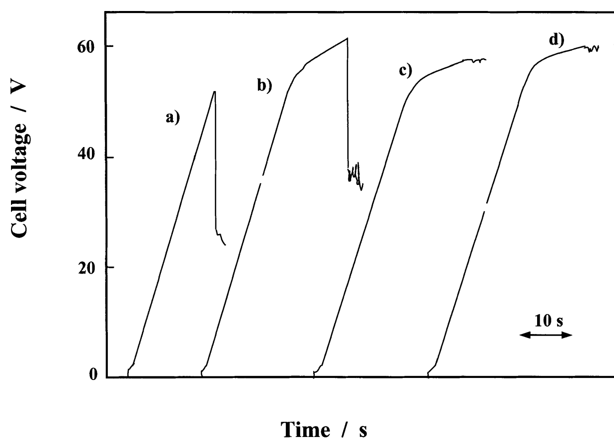

a 1 M HCl; *b* 1 M HCl without (until 35 V) and with (upper part) 0·05 M $FeSO_4$; *c* 1 M HBr; *d* 1 M HNO_3 without (lower part) and with (upper part) 1 M KCl

10 Growth curves of WO_3 anodic films in different solutions at i=8 mA cm^{-2}

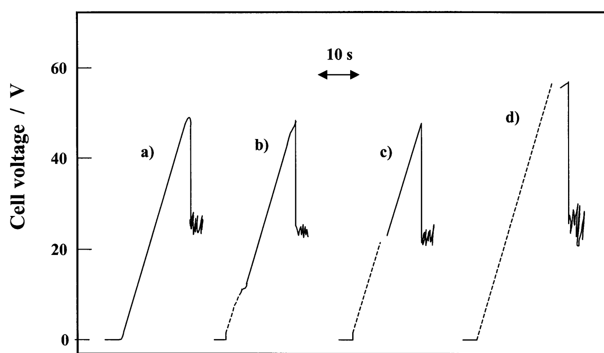

a V_{F1}=0; *b* V_{F1}=10 V; *c* V_{F1}=20 V; *d* V_{F1}=57 V

11 Growth curves in 1 M HCl solution (—) after previous anodisation in 0·5 M H_2SO_4 solution (------) at the same anodising current density of 8 mA cm^{-2} to different voltages V_{F1}

voids during anodising process, has been suggested so that an electromechanical mechanism of breakdown could be invoked in some cases.[58]

As for the electrical breakdown mechanism, there is wide agreement on the influence of both the solid state properties of the passive film and electrolytic contact on the occurrence of such events. This is not surprising because the onset of this phenomenon is sustained by the presence of an electron injection current at the film/electrolyte interface. Thus, it is evident that the understanding of this process, strongly dependent both on the solution composition as well as on the electrical and solid state properties of the passive film on metal electrodes, is preliminary to a quantitative description of the electrical breakdown.

The above mentioned influence is encapsulated in a phenomenological relationship reported many years ago by Gunterschultz and Betz[59]

$$V_b = a + b \log \rho \qquad (23)$$

where V_b is the breakdown potential, ρ the electrolyte resistivity, and a and b are two constants characteristic of the metal – electrolyte couple.

The breakdown potential, also referred to as the first spark voltage V_f, is usually defined as the electrode potential at which large oscillations occur in the growth curve at constant current density, sometimes also accompanied by light emission (sparks) and local crystallisation of the passive film. The phenomenology of this event has been described previously in the literature and will be omitted here.[60]

The prominent role of the solid state properties of the passive film in determining the phenomenology of electrical breakdown rests on the theory of the electronic avalanche mechanism of multiplication of electronic carriers proposed initially to explain the breakdown phenomena in dielectrics.[56] According to this hypothesis, free electron carriers injected into dielectrics are accelerated by the internal electric field and can generate new carriers by impact with ions in the lattice provided that a minimum film thickness pertains. According to this hypothesis, Ikonopisov also suggested that for anodic films the breakdown potential occurs when the electronic current reaches a critical value i_B given by[61]

$$i_B = i_e \exp\left(\frac{reV_b}{e_m}\right) \qquad (24)$$

where V_b is the breakdown voltage, e_m is a threshold energy for impact ionisation and r is a recombination constant of electronic carriers. The term i_e represents the electronic injection current at the passive film/electrolyte interface and it embodies any dependence of V_b on the nature of the electrolytic contact.

As to the nature of the species injecting electrons into the film, several hypotheses have been suggested by different authors and in previous publications,[57,62] the limitations of each one have been discussed by the present authors. In the same work the dependence of V_b on the electrolyte resistivity ρ was explained by taking into account the structure of the passive film/electrolyte interface and the influence of such an interface on the mechanism of oxygen evolution in aqueous solutions. It should be stressed that the proposed model was also able to explain qualitatively some of the reported dependence of V_b on the solution composition and physical parameters. More importantly, the proposed model was able to account for the pitting behaviour of WO_3 in chloride solutions, which was shown to present a dependence on anodising parameters slightly different from that observed for electrical breakdown in solutions not containing chlorides.

Figures 10 and 11 show the influence of various halide ions and an $Fe^{2+/3+}$ redox couple on the breakdown mechanism of an amorphous WO_3 passive film, as well as the absence of any influence of a preformed oxide on the pitting potential of amorphous WO_3. The experimental findings can be summarised as:

1. Pitting of an amorphous WO_3 film during growth at a constant current density occurs only in the presence of a solution containing chloride ions.
2. Electrical breakdown occurs in electrolytic solution containing bromide or iodide species. In the latter case it was necessary to pre-form an anodic oxide film in halogen free solution because of the rapid oxidation of iodide ions occurring at the bare metal electrode.
3. The addition of Fe^{2+} species (as $FeSO_4$) in a limited amount (0·05 M) to 1 M HCl solution shifted the pitting potential significantly (by about 10 V) in the anodic direction, which was anticipated by a phenomenology typical of the onset of an electrical breakdown.
4. The pitting potential of an amorphous WO_3 passive film does not change if an anodic film of variable thickness is preformed in a solution not containing chloride ions, but it pits immediately in solution containing chloride if the film thickness formed in the non-pitting solution is higher than the thickness corresponding to the pitting potential in solution containing chloride (Fig. 11).

All of these findings provide insight on the pitting mechanism of passive films and have been explained by taking into consideration the energetics of the amorphous WO_3/electrolyte interface shown in Figs. 12 and 13. In

CES *(gamma)* CES36636.3d 12/2/04 15:08:14 Rev 7.51n/W (Jan 20 2003)

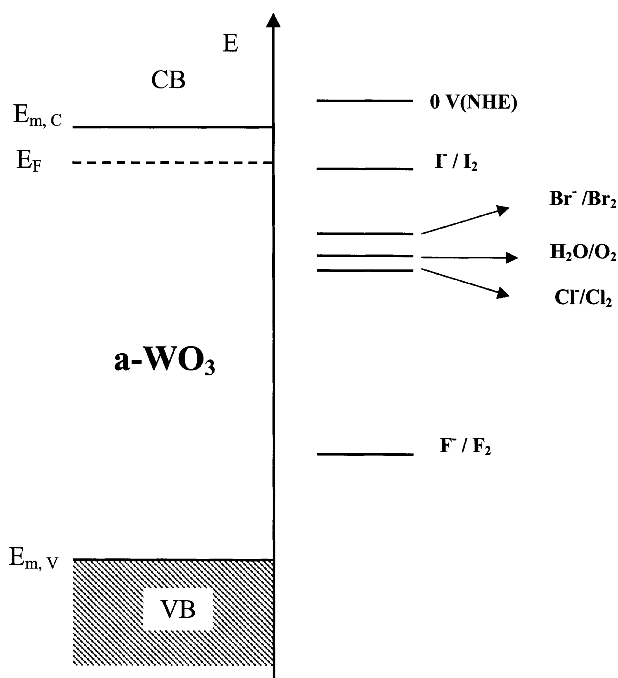

12 Schematic representation of the electron energy levels of amorphous WO_3 and of different redox couples in aqueous electrolyte

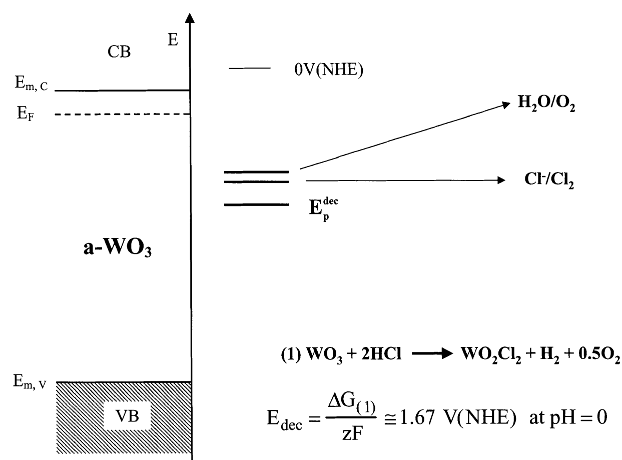

13 WO_3 decomposition level and Fermi level in solution for Cl^-/Cl_2 and H_2O/O_2 redox couple in standard conditions

Fig. 12 the characteristic energy levels of tungsten oxide at pH = 0 as well as the Fermi level in solution for different halide redox couples in their standard state are shown.

According to Gerisher's model of electron transfer at a semiconductor/electrolyte junction, under anodic polarisation no appreciable direct electron injection from halide ions (occupied electronic state in solution) to n type amorphous WO_3 is expected. This is due to the negligible overlapping between full electronic states in solution and vacant extended states in the conduction band of the oxide.

This interpretation is confirmed by the absence of any influence on the electrical breakdown potential of passive films grown in HNO_3 solution containing a small amount (0·05 M) of $Fe^{2+/3+}$ redox couple ($E^\circ = 0{\cdot}77$ V/NHE). It is at variance with the observed decrease of V_b on the addition of the same amount of $Fe(CN)_6{}^{4-/3-}$ redox couple ($E^\circ = 0{\cdot}358$ V/NHE) having a Fermi level in solution nearer to the conduction band of amorphous WO_3. In the latter case, a partial overlapping of filled electronic (red) levels in solution with empty electronic states of the amorphous WO_3 film occurs so that an increase in the electron injection level at the oxide/electrolyte interface owing to the oxidation of $Fe(CN)_6{}^{4-}$ species favours the lowering of V_b by increasing the i_e value in equation (24).

In this frame a rationale for the direct oxidation of I^- species ($E^\circ \geqslant 0{\cdot}54$ V/NHE) across the very thin initial amorphous WO_{3-x} film could be that the initial film on W has a metallic like behaviour or that a direct tunnelling process occurs across this very thin semiconducting oxide. All other halide redox couples having more anodic redox potentials are unable to inject electrons into the conduction band, so allowing the growth of an anodic film with good efficiency.

The growth of amorphous WO_3 in the presence of HBr and HCl solutions is compatible with the electronic properties of the passive films formed in these acids and the good chemical stability of WO_3 against these aggressive anions before the onset of electrical breakdown.

The different behaviour at high potentials, where the breakdown phenomena occur, can be rationalised once again by taking into consideration the energetics of the junction as well as by introducing some consideration of the kinetics of the oxygen evolution reaction (OER) in the presence and in absence of halide ions. Figure 13 shows, for clarity, only the anodic decomposition level of tungsten oxide in the presence of chloride by the formation of soluble tungsten-oxychloride as well as the solution Fermi level for water oxidation. From such a figure it emerges that, in the presence of holes in the valence band of amorphous WO_3, both water oxidation and tungsten oxy-chloride formation are possible anodic reactions competing for hole capture.

On this basis, and by taking into consideration detailed kinetic mechanisms for the oxygen and chlorine evolution reactions it has been suggested[62] that the pitting phenomenon is strictly related to the electrical mechanism of breakdown. In fact the same initial step for electron injection was assumed to be the triggering process for electron avalanche multiplication whilst different reaction pathways are responsible for the onset of electrical or pitting breakdown. The proposed model was able to rationalise the experimental findings including the different dependence of V_{pit} on the experimental parameters.

The beneficial effect of Fe_2SO_4 additions in increasing the pitting potential of WO_3 in 1 M HCl solution is probably related to a scavenger action of Fe^{2+} species towards the generated holes or towards some intermediate in the chloride reaction. The large increase in V_b (about 10 V) in spite of the small addition of sulphate seems to exclude as the source of this effect the possible inhibiting action of sulphate anions. If this suggestion is correct, the effect of the redox couple on the pitting potential value deserves more attention from corrosion scientists with a view to the possible practical application of such effects.

The results described above also rule out the chloride penetration mechanism as a possible explanation for the initiation of pitting on passive tungsten and seem to support a mechanism of local dissolution favoured by the electronic avalanche mechanism of multiplication of electronic carriers.

A local dissolution mechanism involving the formation of soluble Ti^{4+} oxy-halides has also been suggested to account for the different pitting behaviours of TiO_2 passive films in halide-containing solutions.[63] In that work it was suggested that the anomalously low pitting susceptibility of TiO_2 in the presence of Br^- ions could be traced to the strong interaction between these anions and the TiO_2 surface. Such an explanation, although reasonable, suffers from the fact that a regular trend was reported in the pitting behaviour of Zr and Hf parent metals[64] ($V_{pit} > I^- > Br^- > Cl^-$), and is at variance with the finding reported for Ti that the pitting potential increased on going from Cl^- to I^-.

CES (gamma) CES36636.3d 12/2/04 15:08:15 Rev 7.51n/W (Jan 20 2003)

By neglecting the difference in methods for obtaining the pitting potential, the lower pitting potential values reported for these latter metals could be explained along the same lines of reasoning by assuming that a still stronger adsorption of halide ions occurs on insulating ZrO_2 and HfO_2 oxides. Such an assumption could be supported by the hypothesis recently suggested for Al–valve metal alloys that higher concentrations of adsorbed species must be expected at constant potential for passive films having more negative flat band potentials.[65]

The role of U_{fb} values in determining the onset of aggressive halide ion adsorption has also been stressed recently by McCafferty[66] for Al–valve metal alloys on the basis of an indirect correlation between U_{fb} and pH_{pzc} (or isoelectric point) of semiconducting oxides proposed years ago by Butler and Ginley.[67] According to this approach higher pitting potentials should be observed for oxide films having lower pH_{pzc} values or higher U_{fb} values. In this frame the lower pitting potential of $Zr < Hf < Ti$ passive films should agree with the trend in U_{fb} values reported for such passive films (see Table 2 and references therein). Such an approach seems reasonable if the adsorption of pitting promoting anions is controlled by the surface charge at the oxide/electrolyte interface, regardless of whether the triggering mechanism for pit initiation is the local dissolution or the chloride penetration stage.

The generalisation of such a model to the case of Al–valve metal alloys as well as to all semiconducting passive films appears untenable for different reasons. The correlation between oxide electron affinity and flat band potential proposed by Butler and Ginley appears rather limited to a restricted number of oxides. In fact according to the McCafferty data[70] there is no correlation between the flat band potential of TiO_2, ZrO_2, and HfO_2 and their pH_{pzc} values unless some arbitrary correction for the flat band potential values of insulating films or semiconducting ones is invoked.

As for the case of Al–valve metal alloys, the suggestion of semiconducting oxide formation[65] by alloying Al with Ta (known to form insulating oxide like Al_2O_3) or Nb at such low contents is rather surprising. The authors' own data on Al alloying with about 25 at-%Nb or 34 at-%Ta show that anodic films formed on such alloys display insulating behaviour with inversion photocurrent potential values of around $-0{\cdot}64$ V(SCE) and $-0{\cdot}50$ V(SCE) (at $pH = 8$) for Nb and Ta alloying, respectively. In the case of insulating films the inversion potential can be assumed as a measure of the flat band potential in the absence of charge carrier trapping phenomena. It must be mentioned that the present authors' data pertain to films thicker than that investigated in Ref. 65 and used by McCafferty for his correlation.[66]

Moreover, as for the proposed correlation between the band gap of the passive film on Al alloys and V_{pit} in Ref. 66, it must be mentioned that the band gap value ($\cong 3{\cdot}0$ eV) reported in McCafferty's paper for passive aluminium is much lower than that reported in the literature for amorphous Al_2O_3, and has been attributed to the presence of an hydroxide on the aluminium surface formed after mechanical polishing.[71] This last hypothesis is further supported by the fact that anodic films grown on Al–34 at-%Ta and Al–25 at-%Nb alloys display band gap values approximately 4·30 eV and 3·85 eV higher, respectively,[72] than that measured on mechanically treated pure aluminium.

Table 2 Flat band potential (at $pH = 8$) of amorphous passive films grown on different metals

Metal	U_{fb}, V(NHE)	Ref.
Ti	$-0{\cdot}37 \pm 0{\cdot}05$	53
Zr	$-1{\cdot}19 \pm 0{\cdot}1$	68
Hf	$-0{\cdot}60 \pm 0{\cdot}20$	69

CONCLUSIONS

There is no doubt that some meaningful steps toward a better comprehension of the breakdown initiating events have been taken in recent years owing to new experimental and theoretical approaches. It must be concluded, however, that a complete understanding of the breakdown mechanisms is still lacking and that this is particularly true for the pitting initiation mechanism at a microscopic level and its correlation to the solid state properties of the passive films on metals and alloys. However, a deeper understanding of the electronic properties and semiconducting behaviour of passive films will provide new insights into their possible failure mechanisms and the possibility of controlling such catastrophic events.

ACKNOWLEDGEMENTS

This work was financially supported by the University of Palermo.

REFERENCES

1. E. BECQUEREL: *C. R. Hebd. Séan. Acad. Sci.*, 1839, **9**, 561.
2. N. F. MOTT: *Proc. Roy. Soc.(A)*, 1939, **171**, 27.
3. W. SHOTTKY: *Zeits. Physik*, 1939, **113**, 367.
4. W. H. BRATTAIN and C. G. B. GARRETT: *Bell Syst. Tech. J.*, 1955, **34**, 129; *Phys. Rev.*, 1955, **99**, 177.
5. H. GERISCHER: in 'Advances in electrochemistry and electrochemical engineering', (ed. P. Delahay), Vol. 1, 139; 1961, New York, Interscience Publishers.
6. J. F. DEWALD: *Bell Syst. Tech. J.*, 1960, **39**, 615; *J. Phys. Chem. Solids*, 1960, **14**, 155.
7. V. A. MYAMLIN and YU. V. PLESKOV: 'Electrochemistry of semiconductors', 1967, New York, Plenum Press.
8. V. A. TYAGAI and YU. V. PLESKOV: *Elektrokhimiya*, 1965, **1**, 1167.
9. E. K. OSHE and I. L. ROZENFEL'D: *Elektrokhimiya*, 1968, **4**, 1200.
10. R. WILLIAMS: *J. Chem. Phys.*, 1960, **32**, 1505.
11. W. PAATSCH: *J. Phys.*, 1977, **38**, C5–151.
12. E. ANGELINI, M. MAJA and P. SPINELLI: *J. Phys.*, 1977, **38**, C5–261.
13. S. M. WILHELM, Y. ANIZAWA, CHAUNG-YI LIU and N. HACKERMANN: *Corros. Sci.*, 1982, **22**, 791.
14. M. A. BUTLER: *J. Appl. Phys.*, 1977, **48**, 1914.
15. Faraday Discussion No.70, The Royal Society of Chemistry, London, 1980.
16. A. J. NOZIK (ed.): 'Photoeffects at semiconductor-electrolyte interfaces', ACS Symposium Series 146, 1981, Washington, DC, American Chemical Society.
17. S. R. MORRISON: 'Electrochemistry at semiconductor and oxidized metal electrodes', 1980, New York, Plenum Press.
18. F. DI QUARTO, G. RUSSO, C. SUNSERI and A. DI PAOLA: *J. Chem. Soc. Faraday Trans. 1*, 1982, **78**, 3433.
19. U. STIMMING: *Electrochim. Acta*, 1986, **3**, 415.
20. L. PETER: in 'Comprehensive chemical kinetics', (ed. R. G. Compton), Vol. 29, 382; 1989, Oxford, Elsevier Science.
21. 'Passivation of metals and semiconductors', Proc. 5th Int. Symp. on Passivity, (ed. M. Froment), 1983, Oxford, Elsevier.
22. 'Passivation of metals and semiconductors', Proc. 6th Int. Symp. on Passivity, (ed. N. Sato and K. Hashimoto), 1990, Oxford, Pergamon Press.
23. 'Passivation of metals and semiconductors', Proc.e 7th Int. Symp. on Passivity, (ed. K. E. Heusler), 1995, Zurich, Trans Tech. Publications Ltd.
24. 'Passivation of metals and semiconductors', Proc. 8th Int. Symp. on Passivity, (ed. M. B. Ives *et al.*), PV 99-42, 2001, Pennington, NJ, The Electrochemical Society.
25. F. DI QUARTO, S. PIAZZA, M. SANTAMARIA and C. SUNSERI: in 'Handbook of thin films', (ed. H. S. Nalwa), Vol. 2, 373–414; 2002, S. Diego, Academic Press.
26. W. H. LAFLÈRE, R. L. VAN MEIRHAEGHE, F. CARDON and W. P. GOMES: *Surf. Sci.*, 1976, **59**, 401.
27. M. TOMKIEWICZ: *J. Electrochem. Soc.*, 1979, **126**, 1505.

CES *(gamma)* CES36636.3d 12/2/04 15:08:16 Rev 7.51n/W (Jan 20 2003)

28. W. H. LAFLÈRE, R. L. VAN MEIRHAEGHE, F. CARDON and W. P. GOMES: *J. Appl. Phys. D*, 1980, **13**, 2135.
29. G. COOPER, J. A. TURNER and A. J. NOZIK: *J. Electrochem. Soc.*, 1982, **129**, 1973.
30. H. O. FINKLEA: *J. Electrochem. Soc.*, 1982, **129**, 2003.
31. H. GERISCHER and R. MCINTYRE: *J. Chem. Phys.*, 1985, **83**, 1363.
32. S. M. SZE: 'Physics of semiconductor devices', 1969, New York, J. Wiley & Sons, p. 27 of the Italian Edition (1973).
33. P. SCHMUKI and H. BÖHNI: *Electrochim. Acta*, 1995, **40**, 775.
34. M. BÜCHLER, P. SCHMUKI, H. BÖHNI, T. STENBERG and T. MÄNTYLÄ: *J. Electrochem. Soc.*, 1998, **145**, 378.
35. E. SIKORA and D. D. MACDONALD: *J. Electrochem. Soc.*, 2000, **147**, 4087.
36. Y. M. ZENG and J. L. LUO: *Electrochim. Acta*, 2003, **48**, 35.
37. I. DIEZ-PEREZ, P. GOROSTIZ and F. SANZ: *J. Electrochem. Soc.*, 2003, **150**, B348.
38. P. A. COX: 'Transition metal oxides', 1992, Oxford, Clarendon Press.
39. R. DE GRYSE, W. P. GOMES, F. CARDON and J. VENNIK: *J. Electrochem. Soc.*, 1975, **122**, 711.
40. K. UOSAKI and H. KITA: *J. Electrochem. Soc.*, 1983, **130**, 895.
41. H. GERISCHER: *J. Electrochem. Soc.*, 1984, **131**, 2452.
42. R. L. VAN MEIRHAEGHE, E. C. DUTOIT, F. CARDON and W. P. GOMEZ: *Electrochim. Acta*, 1975, **2**, 995.
43. F. CARDON and W. P. GOMEZ: *J. Phys. D Appl. Phys.*, 1978, **11**, L63.
44. F. DI QUARTO, C. SUNSERI and S. PIAZZA: *Ber. Bunsenges. Phys. Chem.*, 1986, **90**, 549.
45. F. DI QUARTO, V. O. AIMIUWU, S. PIAZZA and C. SUNSERI: *Electrochim. Acta*, 1991, **36**, 1817.
46. F. DI QUARTO, S. PIAZZA and C. SUNSERI: *Electrochim. Acta*, 1990, **35**, 99.
47. J. D. COHEN and D. V. LANG: *Phys. Rev. B*, 1982, **25B**, 5321.
48. D. V. LANG, J. D. COHEN and J. P. HARBISON: *Phys. Rev. B*, 1982, **25B**, 5285.
49. R. A. ABRAM and P. J. DOHERTY: *Philos. Mag. B*, 1982, **45**, 167.
50. I. W. ARCHIBALD and R. A. ABRAM: *Philos. Mag. B*, 1983, **48**, 111.
51. I. W. ARCHIBALD and R. A. ABRAM: *Philos. Mag. B*, 1986, **54**, 421.
52. I. W. ARCHIBALD and R. A. ABRAM: *Philos. Mag. B*, 1987, **56**, 429.
53. S. PIAZZA, C. SUNSERI and F. DI QUARTO: *A.I.Ch.E. J.*, 1992, **38**, 219.
54. F. DI QUARTO and M. SANTAMARIA: Proc. Symp. on 'Surface oxides'; 204th ECS Meeting, Orlando, FL, October 2003. Submitted. 1
55. Z. SZKLARSKA-SMIALOWSKA: *Corros. Sci.*, 2002, **44**, 1143.
56. F. DI QUARTO, S. PIAZZA and C. SUNSERI: *J. Electrochem. Soc.*, 1984, **131**, 2901.
57. F. DI QUARTO, S. PIAZZA and C. SUNSERI: *J. Electroanal. Chem.*, 1988, **248**, 99.
58. H. HABAZAKI, M. UOZUMI, H. KONNO, K. SHIMIZU, S. NAGATA, K. ASAMI, K. MATSUMOTO, K. TAKAYAMA, Y. ODA, P. SKELDON and G. E. THOMPSON: *Electrochim. Acta*, 2003, **48**, 3257.
59. A. GUNTERSCHULTZ and H. BETZ: 'Electrolyt-Kondensatoren', 116; 1952, Berlin, Technischer Verlag Herbert Cram.
60. D. A. VERMILYEA: in 'Advances in electrochemistry and electrochemical engineering', (ed. P. Delahay), Vol. 3, 211; 1963, New York, Interscience Publishers.
61. S. IKONOPISOV, A. GIRGINOV and M. MACHKOVA: *Electrochim. Acta*, 1977, **22**, 1077.
62. F. DI QUARTO, S. PIAZZA and C. SUNSERI: *J. Electroanal. Chem.*, 1988, **248**, 117.
63. S. B. BASAME and H. S. WHITE: *J. Electrochem. Soc.*, 2000, **147**, 1376.
64. S. HORNKJOL: *Electrochim. Acta*, 1998, **33**, 289.
65. J. O'M BOCKRIS and Y. KANG: *J. Solid State Electrochem.*, 1997, **1**, 17.
66. E. MCCAFFERTY: *Corros. Sci.*, 2003, **45**, 301.
67. M. A. BUTLER and D. S. GINLEY: *J. Electrochem. Soc.*, 1978, **125**, 228.
68. F. DI QUARTO, S. PIAZZA, C. SUNSERI, M. YANG and S.-M. CAI: *Electrochim. Acta*, 1996, **41**, 2511.
69. F. DI QUARTO, M. SANTAMARIA, P. SKELDON and G. E. THOMPSON: *Electrochim. Acta*, 2003, **48**, 1143.
70. E. MCCAFFERTY: *J. Electrochem. Soc.*, 1999, **146**, 2863.
71. F. DI QUARTO, G. TUCCIO, A. DI PAOLA, S. PIAZZA and C. SUNSERI: *Proc. Electrochem. Soc.*, 1994, **94-25**, 25.
72. M. SANTAMARIA and F. DI QUARTO: Proc. Symp. on 'Surface oxides': 204th ECS Meeting, Orlando, FL, October 2003. Submitted. 2

CES *(gamma)* CES36636.3d 12/2/04 15:08:17 Rev 7.51n/W (Jan 20 2003)

AUTHORS QUERIES

Journal: **Corrosion Engineering, Science and Technology**
Paper: **2127**

Dear Author
During the preparation of your manuscript for publication, the questions listed below have arisen. Please attend to these matters and return this form with your proof. Many thanks for your assistance

Query Reference	Query	Remarks
1	Author: Please update Ref. 54.	
2	Author: Please update Ref. 72.	